SNDICE: a direct illumination calibration experiment at CFHT

C. Juramy[a], E. Barrelet[a], K. Schahmaneche[a], P. Bailly[a], W. Bertoli[a], C. Evrard[a], P. Ghislain[a]
, A. Guimard[a], J.-F. Huppert[a], D. Imbault[a], D. Laporte[a], H. Lebbolo[a], P. Repain[a], R. Sefri[a],
A. Vallereau[a], D. Vincent[a], P. Antilogus[a], P. Astier[a], J. Guy[a], R. Pain[a], N. Regnault[a],
R. Attapatu[b], T. Benedict[b], G. Barrick[b], J.-C. Cuillandre[b], S. Gajadhar[b], K. Ho[b], D. Salmon[b]

[a]Laboratoire de Physique Nucléaire et de Hautes Énergies, 4, place Jussieu, 75252 Paris, France;
[b]CFHT Corporation, 65-1238 Mamalahoa Hwy, Kamuela, Hawaii 96743, USA

ABSTRACT

We present the first results of the SuperNova Direct Illumination Calibration Experiment (SNDICE), installed in January 2008 at the Canada France Hawaii Telescope. SNDICE is designed for the absolute calibration of the instrumental response of a telescope in general, and for the control of systematic errors in the SuperNova Legacy Survey (SNLS) on Megacam in particular. Since photometric calibration will be a critical ingredient for the cosmological results of future experiments involving instruments with large focal planes (like SNAP, LSST and DUNE), SNDICE functions also as a real-size demonstrator for such a system of instrumental calibration. SNDICE includes a calibrated source of 24 LEDs, chosen for their stability, spectral coverage, and their power, sufficient for a flux of at least 100 electron/s/pixel on the camera. It includes also Cooled Large Area Photodiode modules (CLAPs), which give a redundant measurement of the flux near the camera focal plane. Before installing SNDICE on CFHT, we completed a full calibration of both subsystems, including a spectral relative calibration and a 3D mapping of the beam emitted by each LED. At CFHT, SNDICE can be operated both to obtain a complete one-shot absolute calibration of telescope transmission in all wavelengths for all filters with several incident angles, and to monitor variations on different time scales.

Keywords: Photometry, Calibration, LED, Telescope

1. INTRODUCTION

The latest results of experiments using type Ia supernovae as standard candles showed a crucial need for a photometric calibration with an accuracy below 1 % [1]. The next generation of wide-field imagers will absolutely need such an improved calibration. The uncertainties of the photometric measurements are related to atmospheric absorption and to the instrumental telescope calibration. The SNDICE device aims to improve this instrumental calibration with a new concept [2]: the direct illumination of the primary mirror using stable, point-like sources.

This device was conceived in 2007. We report on the design of the device, its calibration on our photometric and spectroscopic benches and, finally, on the installation at CFHT in Hawaii and the preliminary analysis of the first data set.

2. HARDWARE

2.1 LED source

2.1.1 Light beam

From the start, the SNDICE concept was built around the choice of LEDs as light sources. LEDs have the flexibility to emit a wide range of programmable fluxes with programmable durations, great stability of their emissions over time, and the correct spectral properties (bandwidth and wavelength coverage) to study the instrumental response of a CCD camera and its filters. Twenty-four LEDs have been selected for SNDICE

(Send correspondence to C.J.: E-mail: juramy@lpnhe.in2p3.fr, Telephone: +33 (0)1 44 27 45 80)
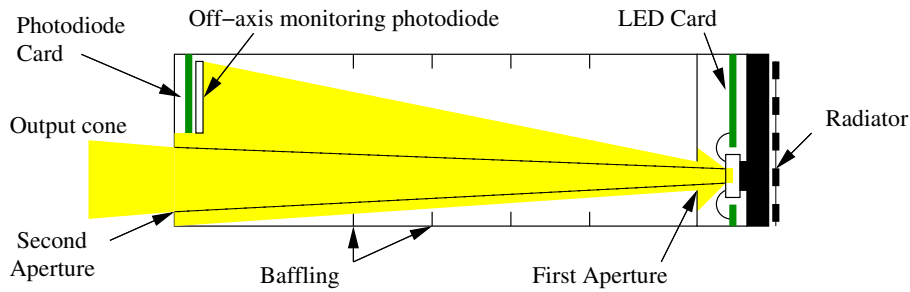
Figure 1. One LED channel, showing the path of LED light from the emitting surface to the second aperture (defining the 'useful' light cone) and to the monitoring photodiode. Baffling was added to block stray light.
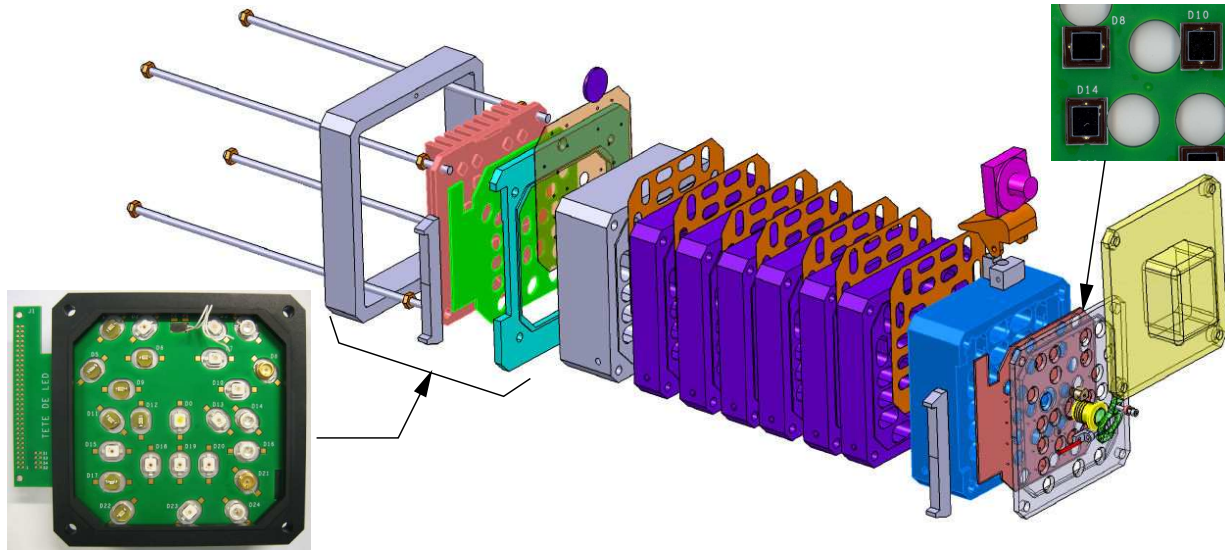
Figure 2. Final mechanical drawing of the LED source and pictures of the LED board (left) and the monitoring photodiodes (right). The artificial planet is placed at the axis of symmetry of the source. The webcam on top gives us a view from the vantage point of the source.

'LED source', covering most of the Megacam bandwidth (see spectra on Figure 8). These LEDs vary greatly in efficiency and maximum current (between 20 mA for the bluest UV LEDs and 500 mA for 'Golden Dragon' OSRAM LEDs). Their spectra, measured on the spectral test bench (section 3.5), are smooth as expected, except for the reddest LEDs in the near-IR.

The LED source mechanical design (fig. 2) fits the 24 calibration beams and the 'artificial planet' channel (described in 2.1.3) within a 12x12x28 cm block, divided in slices for assembly. The output beam for each LED is defined by the emitting surface of the LED and two circular apertures (fig. 1), with respective diameters of 2 and 10 mm. The first aperture is necessary for baffling, the second aperture defines the shape of the beam as a cone with a summit angle of $2°$, an angular size sufficient to cover the whole field of Megacam when illuminating the telescope. Each slice of the body of the source is anodized to decrease light reflexions inside each channel. Between slices, baffling masks are inserted to eliminate light reflecting at grazing angles. It is essential to insure good thermalization of the LED despite the high power dissipation. This is obtained by gluing the LED heat sinks directly to the radiator block. The webcam atop the LED source is a very useful tool for rough alignment and diagnostic purpose, since the access to the LED source is limited when mounted on the dome of the telescope.

2.1.2 Off-axis monitoring photodiodes

As shown Figure 1, a photodiode (Centronic OSD35-7CQ) is placed off-axis inside each calibration channel, on a board positioned right before the second aperture (see also fig. 2). This photodiode provides monitoring
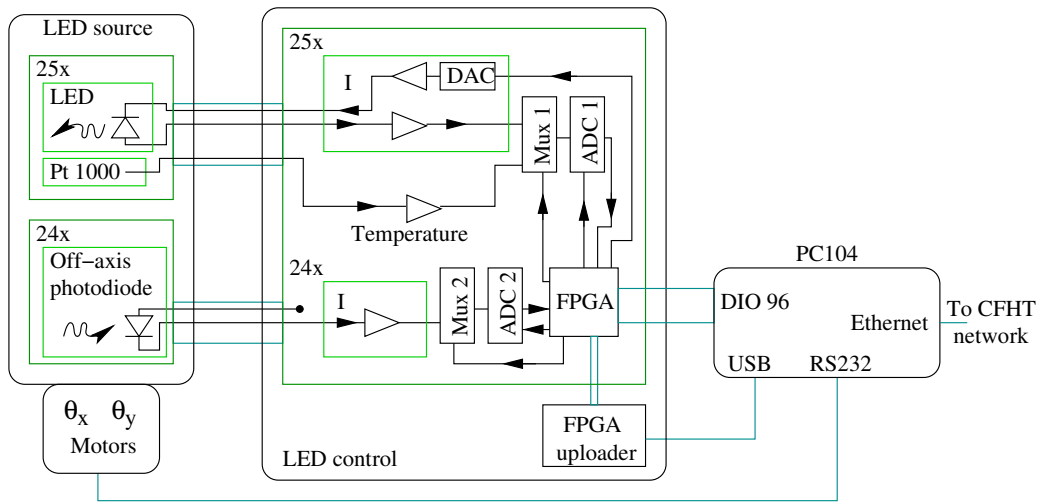
Figure 3. Block diagram for the LED source, including all elements of the back-end board.

of the light output of the LED as a function of time and input current. The current amplifier used for these photodiodes is an AD549JH with a $1\,M\Omega$ feedback resistor*. In addition to the direct measurement of the LED current, the monitoring photodiodes are the first key to check the stability of the calibration beams, the second key being the CLAP (see section 2.2).

2.1.3 Alignment channel: the 'artificial planet'

A 'white' LED is positioned at the center of the source, with a pinhole (50μm) at the level of the first aperture and a lens (focal length 25 cm, diameter 11 mm) placed at the level of the second aperture(see fig. 2). The distance between the pinhole and the lens is adjusted mechanically to yield a parallel beam. We use this channel of the source both on the calibration bench and on the telescope to align the LED source (see section 4.2.2). We call it the 'artificial planet'[†], because the beam is focused by the primary mirror into a spot covering approximately 250 pixels on Megacam, as expected given the size of the pinhole. The spectrum of the 'white' LED is limited to the visible spectrum (as seen fig. 8) and does not cover the whole spectrum of interest. Therefore the alignement between the SNDICE source and the telescope using the artificial planet is usually done without filters.

2.2 CLAP

The detector of the CLAP module is a Hamamatsu photodiode (S3477-04) with an integrated Peltier cooler. Its sensitive surface is a square with a side of 5.7 mm. The current passing through the cooled photodiode is read on a 'front-end card' inside the CLAP module, which acts as a shield against pick-up noise on the signal lead. The readout is done by our Low Current Amplifier ASIC [3], with an external feedback resistor of either $100\,M\Omega$ or $1\,G\Omega$, depending on the desired range. The current amplifier is followed by a voltage amplifier of factor 20.

The single stage Peltier cooler lowers the temperature of the photodiode by -35°C. A thermal sensor (resistor) is included in the photodiode packaging. The front-end card also generates the voltages for the polarization of the photodiode (1.5 V) and for the thermal sensor.

2.3 Back-end electronics

Each of SNDICE subsystems is commanded through a back-end board, based on the same core design (fig 3). One CLAP back-end board can accommodate up to 4 CLAP front-end modules. Commands and readouts are managed by an Altera FPGA, with a clock running at 1 MHz to control start times and pulse durations. A 14-bit DAC controls the current in each LED for the LED source, and the same current amplifiers are used to

---

*The flux emitted by each LED being measured, we can tailor the feedback resistor to the LED power in each channel.
[†]By contrast to an 'artificial star', used in testing detectors, which has a beam focused to below the size of a pixel.

generate Peltier cooling for the CLAPs (up to 500 mA per LED, 1 A per CLAP). In the LED source, two 32-channel multiplexers are followed by two 16-bit ADCs to read out the current in the LEDs and in the monitoring photodiodes. In the CLAP back-end, one multiplexer followed by one ADC measures the CLAP output voltage after amplification of the current, and the voltage from temperature monitoring.

3. CALIBRATION BENCH

3.1 Principles

The goal of the calibration bench is to measure with a high precision (below the per mil):
- the light fields of each LED at a given current (3D mapping of the beam),
- the variations of these fields as a function of the current in the LEDs,
- the stability of the emission as a function of time (total flux and spectra),
- the response of the CLAP as a function of the wavelength.

Starting with a NIST (National Institute of Standards of Technology) and a DKD (Deutscher Kalibrierdienst) Gigahertz Optik calibrated photodiodes we transfered the absolute calibration of these two detectors to the LEDs then from the LEDs to the CLAP. This is done in several steps and several configurations of our calibration bench. Considering the stability of the LED emissions and the precision of measurements, the accuracy of LED calibration is presently limited by that of the detectors.

The 'photometric calibration' is done using a kind of light-luminosity measurement. Using precise motorisation we map the light field at different distances of the light source, and we compare the fluxes measured by a standard detector and the CLAP. This 'photometric bench' has two configurations: one short-range with the photodetectors located between 1.15 m and 2.5 m and a second long range with distances of the order of 14 m. The first bench allows a mapping of the entire field and its edges, the second is focused on only a small part of the field but at a distance which can be fixed to the CFHT focal length.

The spectral calibration compares the light flux of a given LED at the output of a spectrometer measured by a standard detector and the CLAP. This procedure allow us to measure the spectra of the LEDs and measure the response of the CLAP.

3.2 Overview

For calibration operations, the whole 2.5 m bench is enclosed in a 'black box'. A 12 m-long tube is extended from the black box to create a bench up to 14.5 m in length. The source is at a fixed position, inside the black box for the short range bench, and at the entrance of the tube for the long range bench. The moving part of the bench is the common mount holding one CLAP and one calibrated photodiode (read out with a 6514 Keithley picoammeter). The 3D motorization includes a 1.5 m-long Z axis for movement parallel to the source axis, and 30x30 cm XY axes for movements in the perpendicular plane, sufficient to cover every beam from the source (each approximately 9 cm in diameter at 2.5 m).

LabVIEW software was used to control all elements of the calibration bench, and to automatize calibration operations. Aside from linearity checks, most tests were done for a few selected values of LED current, chosen as follows: close to the maximum rating for low-power LEDs to have as much flux as possible, covering a wide range (between 5 and 75 %) for high-power LEDs to test both the highest fluxes available and fluxes matching the low-power LEDs.

3.3 Photometric calibration: angular mapping

The primary goal of the operations on the photometric bench is the absolute calibration of the beams emitted by the 24 LEDs. Since the beams show some irregularities at the percent level, the calibration has to perform an angular mapping of each beam, and to check that it is independent of the distance. In addition to local features, the beams from some LEDs show a slope across the 'flat' area, caused by a partial masking of the LED emission surface by the first aperture (it will be eliminated in the next generation of the LED source). We fit this slope with a plane using the most precise full scan. To quantify the reliability of this mapping, we look at the residuals after subtraction of this plane for scans at 4 different distances (accounting only for the distance
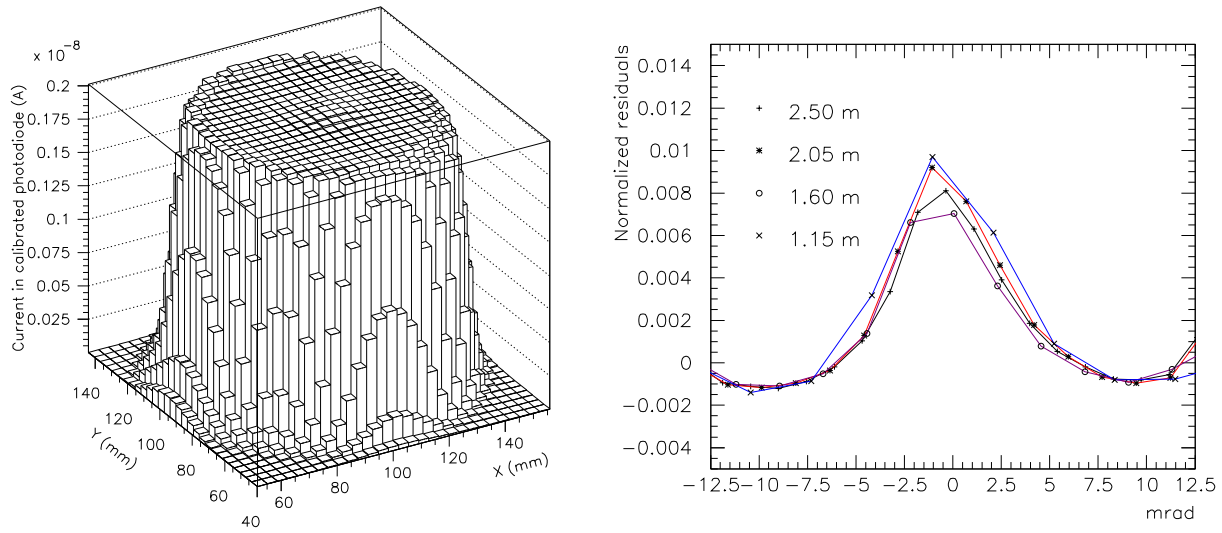
Figure 4. 3D mapping of the field. Left: Mapping of the beam of one Golden Dragon LED (with a calibrated photodiode of 3.5*3.5 mm at 2.5 m). The 'flat field' cylindrical region, being slightly inclined, is fitted with a plane. The residuals consist of a central 'bump', 1 % of flat field current in amplitude, which is intrinsic to the LED. The 'rim' at the edge of the beam is caused by the first aperture. Right: Independence of the central bump from the distance. The similarity of the residuals at four different distances (after conversion to angular size and subtraction of the underlying plane) shows the reliability of the beam model.
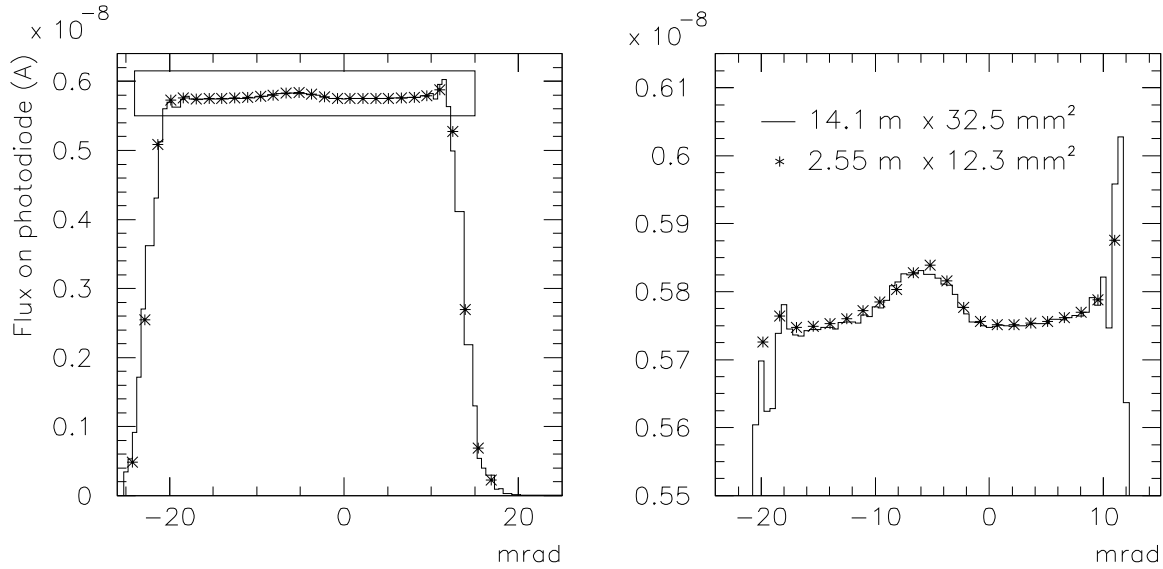
Figure 5. Matching between a 2D map at 2.5 m and an angular scan at 14 m. The normalization factor of 12.0 applied to the long range data is due to the difference in photodiode size (0.379, calculated through fitting on the short range bench) and the inverse squared distance factor (from 2.55 to 14.1 m).
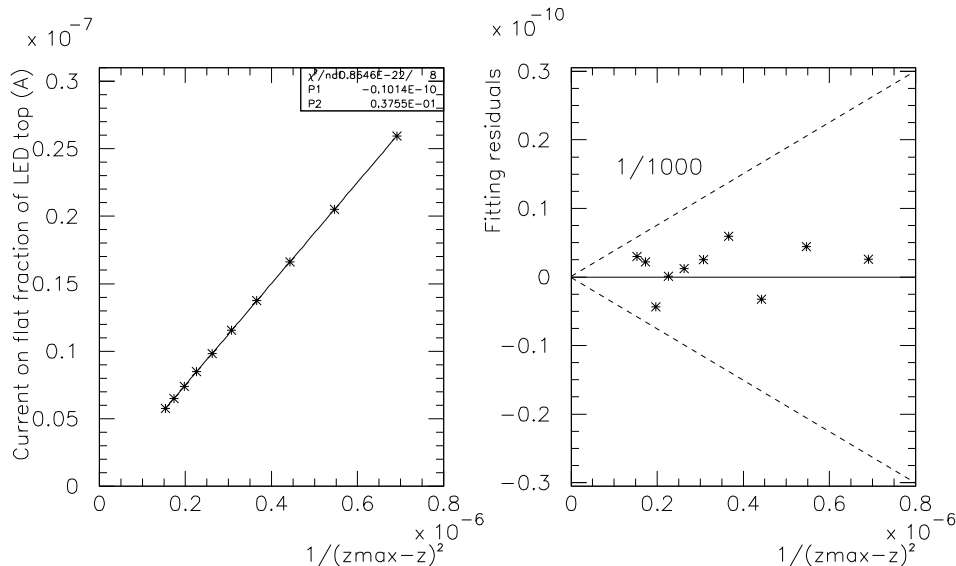
Figure 6. Fit of the flux in the calibrated photodiode as a function of the inverse square of the distance from the source (with the maximum distance fixed at 2,553 mm). The flux value was estimated in each case on the 'flat' part of the beam.

factor between them). As shown Figure 4, we find that the residuals are identical to 1 per 1000, with the paving size causing the differences on the slopes around the central feature.

Due to the size of the beam at long range (around 45 cm), we are limited both by the diameter of the 12-m tube (30 cm), and by the time a full scan would take. Instead of a full scan, we used the angular motors to do a fine scan in two directions on one beam, by moving the LED source relatively to photodiodes, positioned at the estimated center. The main goal of these scans was to test the compatibility of the beam geometry at short range and at long range, with a positive result (fig. 5).

3.4 Photometric calibration: absolute calibration and light-to-distance relation

Once the irregularities are accounted for as residuals to a model, which can be a 'flat' value in the ideal cases, and a plane in any case, the parameters of the model are sufficient to describe the beam. The values of the parameters obtained from the scans are then used for the absolute calibration (as in fig. 6). This is done for all beams using the four different distances (between 1.15 and 2.5 m), and using ten different values for one to check the method more extensively, including the determination of the exact distance between LED source and the Z axis reference. Doing the 10-distance series for the two sizes of calibrated photodiode, we found a ratio of 0.379 between them. This result is convincingly close to the nominal geometrical ratio of 0.377, which is only an approximation of the real ratio of collecting surfaces.

For the calibration at long range, the main issue created by the limited diameter of the tube is the reflexions on the inside. We added baffling to suppress these reflexions, in the shape of a circular aperture 5 cm in diameter, at 5 m from the source. This cuts off most of the beam, leaving only a selected spot at the level of the photodiodes, at a position depending on the position of the LED relative to the center of the source. We repeated for these spots the same type of mapping as on the short range bench, with 4 distances for all LEDs and 10 distances for 2 LEDs. At this long range, the best method for an exact measurement of the distance is still the comparison with a short-range scan, as done Figure 5.

The long range bench is also the best setup to test the LEDs and CLAPs in flux ranges matching those expected when mounted on a telescope. This includes the cross-calibration of all CLAP ports on the two back-end cards (prototype and final), and linearity measurements at several levels (linearity of LED flux relative to LED current, of CLAP output relative to LED flux, of CLAP digital output relative to voltage output).
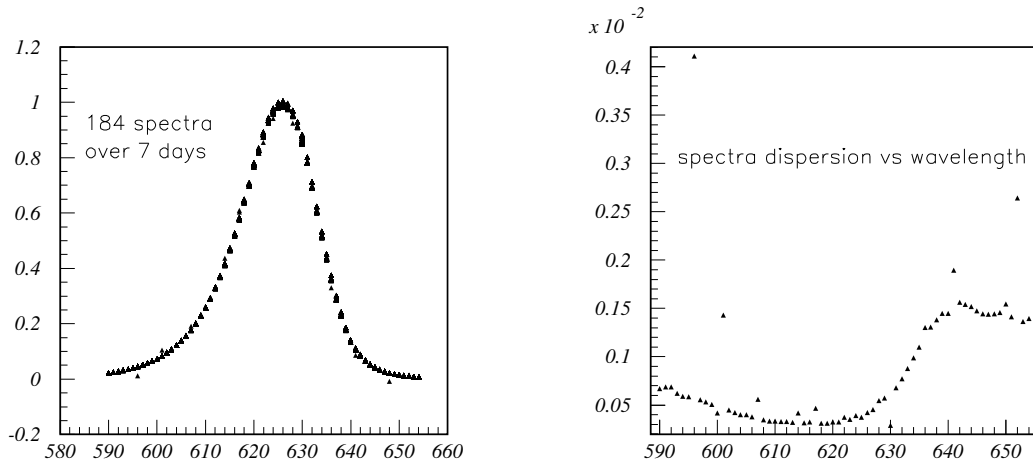
Figure 7. Stability of a LED spectra: 184 spectra were taken over 7 days with the same level of the current in the LED. The maximum dispersion of the normalized spectra is found at the red edge, and stays below 0.2 %, corresponding to a 0.01 nm shift in wavelength.

3.5 Spectral calibration

The spectral calibration was done by positioning each LED in turn in front of the input slit of a monochromator. We then used the vertical axis to position in turn the calibrated photodiode and the CLAP at the output slit, to do a relative spectral calibration on the combined spectrum of all LEDs. The majority of LED spectra varied by less than a few nanometers on the range of 5 to 75 % of maximum current. At a given current, we measured a stability of the spectra below 0.2% (fig. 7).

4. HAWAII CHFT RUN

4.1 Installation of SNDICE for MegaCam calibration

MegaCam is for the moment the largest existing imager with thirty-six $2k \times 4k$ CCDs covering a total field of view of 1 square degree. It is located at the primary focus of the Canada France Hawaii Telescope, which primary mirror has a 3.6 m diameter and an equivalent focal length of 13.6 m. Following the path of incoming light after the mirror, we find the Wide Field Corrector, consisting of several lenses, then the filter, and the cryostat window, all located just in front of the CCDs. The goal of SNDICE is to study and monitor the efficiency of MegaCam and the transmission of CFHT optical elements, including the 5 Sloan filters used by SNLS : u*, g', r', i', z' (Figure 9).

4.1.1 Hardware

Inside the CFHT dome are two stairways leading up to the platforms located at $\pm 108°$ from the dome slit (fig. 10). The East platform is now hosting the LED source and all associated hardware. The LED source itself with its angular motors is mounted on an arm extending from the back of the platform (fig. 10), which is in turn bolted to a platform strut and leveled within 0.1° of horizontality. When the telescope is pointed towards the LED source, its elevation is 59°. A scan within a $\pm 8°$ angle around this direction enables to cover the whole surface of the mirror. The platform has been equiped with a bay to hold and to protect the electronics, a remote power control, a webcam, and an ethernet link established through the AC supply.

Two CLAPs were placed on the primary mirror support ('caisson central'), on the support beam used by the Sky Probe[‡], side by side, and inside a box for baffling. The back-end electronics and computer are placed

---

[‡]A camera which provides a measurement of the atmospheric attenuation.
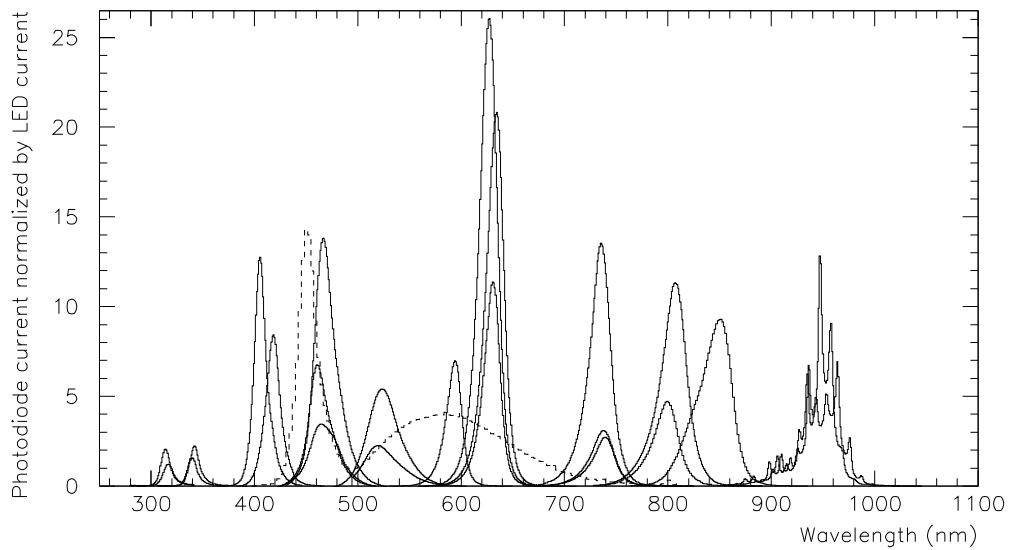
Figure 8. Spectra of all LEDs selected for the LED source. The measured current is normalized by the input LED current, both in their own ADU scales. The difference between two LEDs at a given wavelength is therefore only due to differences in emission efficiency. The spectrum of the 'white' LED (dashed line), used for the artificial planet, was multiplied by 50 to compensate for its wide spectrum.
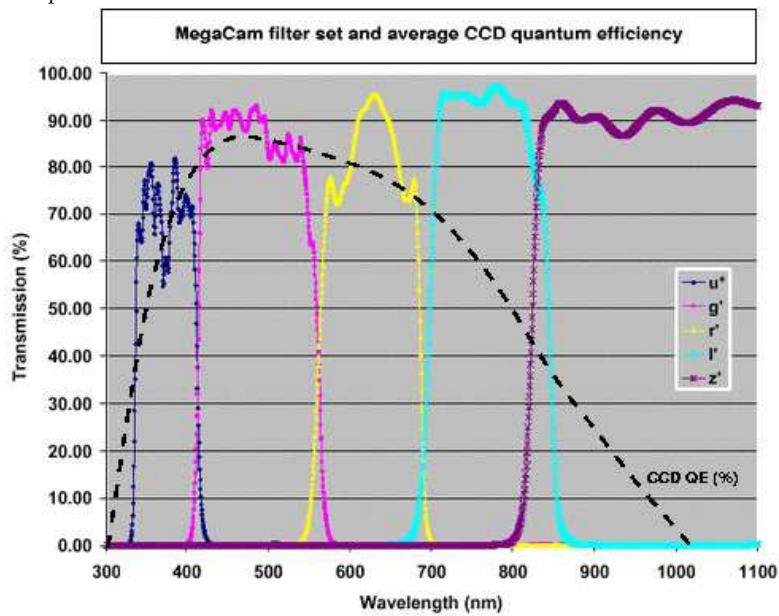
Figure 9. Megacam ugriz filter set and mean quantum efficiency of the CCDs: responses as a function of the wavelength.
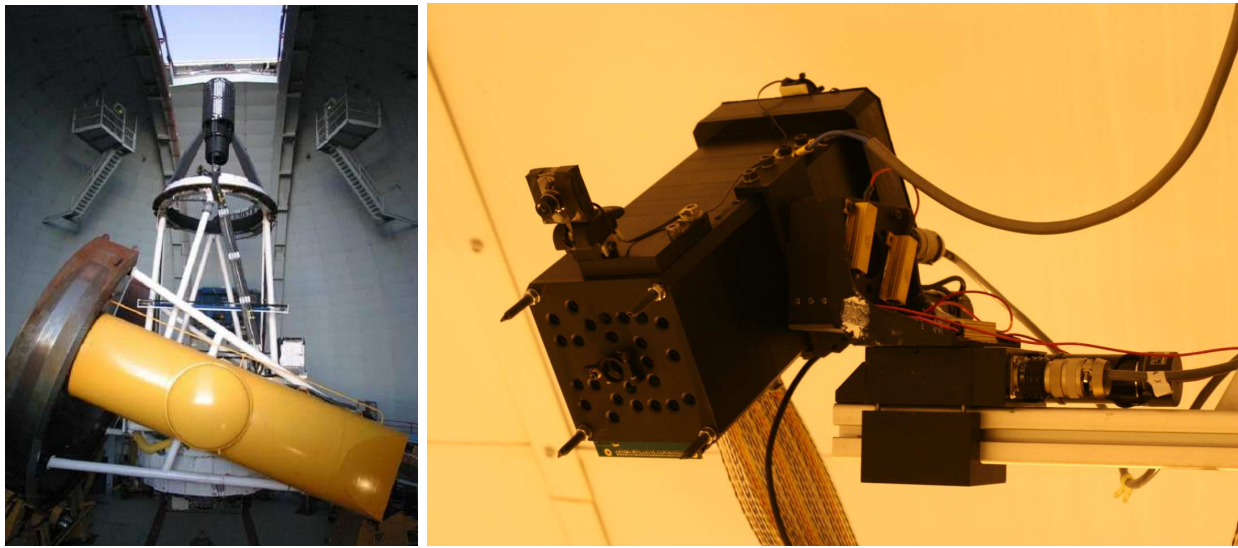
Figure 10. Installation of SNDICE in the CFHT dome. Left: overall view inside the dome, showing the platforms and the dome slit. Right: SNDICE LED source mounted on the platform.

nearby, inside a bay. If we target the CLAPs instead of the mirror, we obtain a direct check of the LED flux at this distance, before it goes into the optics. The next extensive maintenance operation will make it possible to install one CLAP close to MegaCam shutter.

4.1.2 Software

One PC 104[§] controls each side, LED source and CLAPs. Both are connected to the CFHT network, and can be booted and controlled remotely. Software maintenance can also be done remotely, including download of updated FPGA programming. Both computers are running a server (a LabVIEW program), which handles commands sent to the instruments and data retrieval. This has been integrated to the CFHT software architecture, in which sequences of commands are sent to the different subsystems. Calibration procedures can either be controlled manually, sending each command to the source, the camera, the filter, etc., or by prepared sequences.

4.2 Preliminary run

4.2.1 Data set

SNDICE calibration data can be accumulated at any time of the day, or at night when the dome is closed due to the weather. This first data set was taken in a few hours in February 2008, consisting of both 'artificial planet' and calibrated LEDs shots, with and without filter in front of Megacam. These data allowed us to define the alignement procedure of SNDICE with respect to the telescope and to do a first calibration study of Megacam. With a device such as SNDICE (ie : a point like source but at a finite distance), each pixel 'sees' only one light path to the LED. To be able to scan the whole aperture of the telescope, we cycle through different positions of the light spot on the primary mirror.

4.2.2 Alignment

The preferred position for calibration is obtained when the optical axes of SNDICE and the telescope are aligned, or equivalently when the spot of the 'artificial planet is located at the center of the CCD mosaic. During the first run, this alignment was achieved by trial and error, moving SNDICE. The precision obtained is ±10", half of the apparent diameter of the artificial planet (40"). This data was then used to compute the parameters of the geometrical model of the relative movements of the telescope and of SNDICE source [4], which uses the telescope reference system for SNDICE targeting. This model will be incorporated into a dedicated program for faster alignment procedures in future calibration runs.

[§]PC units designed for embedded applications.
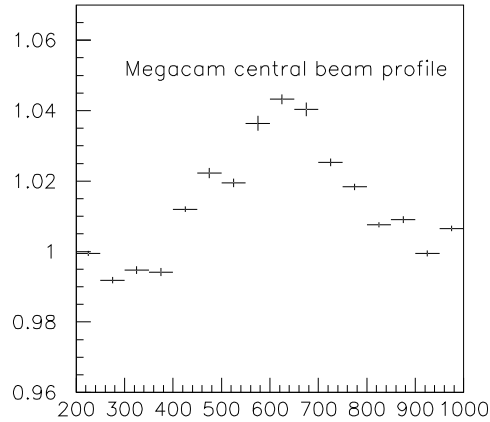
Figure 11. Central 'bump' of a LED beam measured by Megacam. It is a single image rebinned in superpixels (16x16). Some diffraction patterns are still present and prevent from having a more flat background. A simple normalisation of each CCD/amplifiers has been done by continuity.

4.3 Preliminary CFH calibration

The incomplete set of calibration data taken during the first run allows us to highlight already several potentialities of SNDICE. As the light source is at a finite distance of the telescope, each Megacam pixel is reached by a given light ray. And if there is an obstacle on the light path of this ray, it yields a diffraction pattern on the CCD. To reject these patterns, we take several images with different positions of the LED beam on the primary mirror but always with parallel optical axes, and then, in this first preliminary analysis, we build a median frame from, typically, 10 images.

It is possible to check that the LED beam seen by Megacam shows the same central feature as the 3D mapping from the calibration bench (fig. 11).

4.3.1 Gain control and filter transmission

The flatness and the stability of the LED beam allows to have a control of the stability of the amplifier gains (fig. 12). It allows also to measure the spatial variations of filter transmissions. We only have to divide images taken with a given LED with and without a given filter.

For example, one can see very clearly using the LEDs corresponding to the g' filter an inefficiency of this filter in the center of the camera (fig. 12), confirming a previous analysis made for SNLS on dense fields of stars. Another striking example is the i' filter (fig. 13). Here, the transmission of the filter is uniform for LED wavelengths well inside the filter bandpass, but not at all for a LED at the edge of the filter bandpass, suggesting a non-uniformity of this filter bandpass.

4.3.2 Double Fresnel reflexions

SNDICE allows to study light reflexions in the differents optical elements surrounding the camera. By selecting a LED whose central wavelength is close the edge of a filter, one highlight reflexions between the filter and the surface of the last lens of the Wide Field Corrector (fig. 14). It gives a pincushion-shaped pattern. This is the result of a square beam reflecting first from any of the flat surfaces above the corrector then reflecting from the curved surface of the final lens in the corrector. A ray tracing simulation gives the same shape (right in fig. 14). The contribution of this reflexion is amplified by the concentration of the whole beam into a smaller region near the center. This example shows that contrary to simple intuition, correcting for the reflexions is not negligible
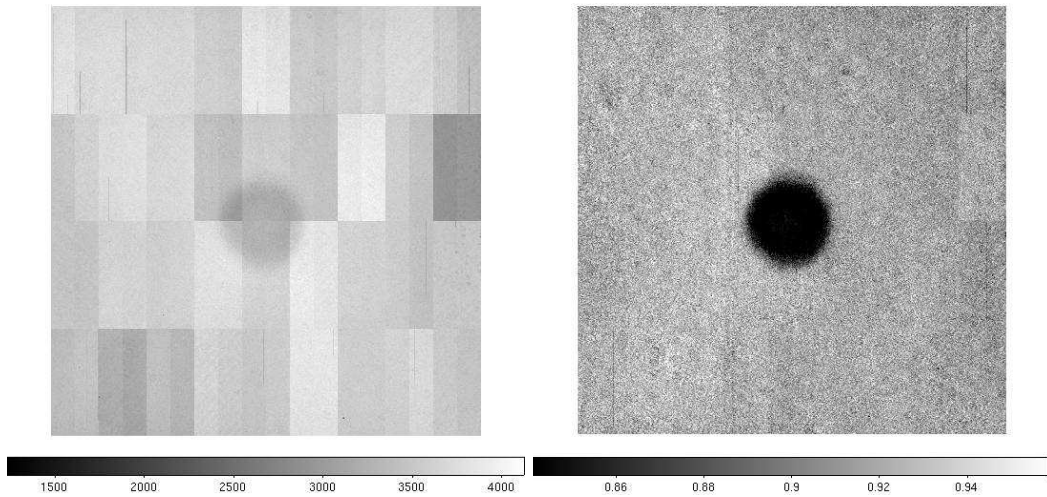
Figure 12. A 480 nm LED illuminating the mosaic with the filter g' in front of the CCDs (left). One can see the different gains of various amplifiers. And by making the ratio of that image with one taken without any filter, we obtain the g' filter transmission (right), showing an inefficiency of 10 % in the center.
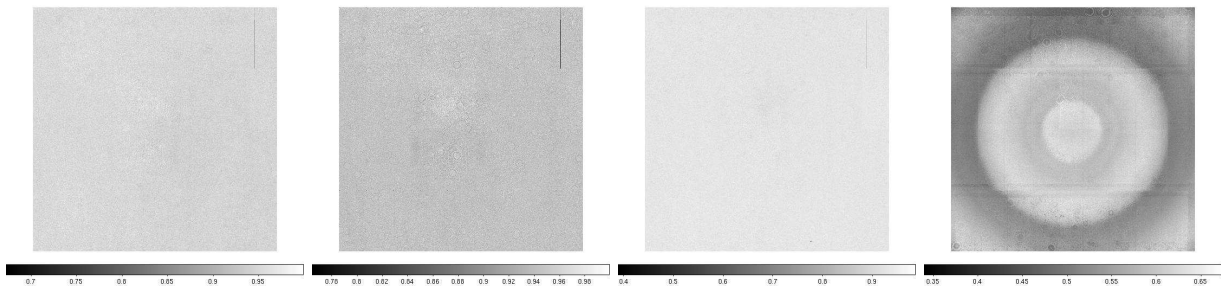
Figure 13. i' filter observed with 735nm, 750nm, 810nm and 850nm LEDs. One can see very clearly the features appearing with the 850nm LED, which is at the edge of the filter bandpass.

nor trivial. These reflexions appear clearly in the direct illumination setup of SNDICE, but they could also be present when using 'flat-fielding' techniques, creating an illumination contrast between the center and the sides of the mosaic.

5. CONCLUSION

While we have shown the ability of SNDICE to characterize filter transmission and bandwidth, we have also demonstrated at a stroke that non uniformity is a fact of life with wide field instruments (a fact appearing also in SNLS calibration from a long and complex analysis of dense star fields). Moreover we discover at our own surprise that, due to large angle optics, Fresnel reflection effects are not necessarily small, nor uniform. It is still a far cry from recalibrating ab initio a complex instrument like Megacam, but it is clear that it will bring a new lever arm to make their analysis more powerful.

By crossing our Megacam data with our calibration bench data and SNLS star calibration data, we should be able to tackle absolute calibration of both the reference stars and the Megacam instrument. A fascinating fact on this path is the $< 0.1\,\%$ stability of our LED source, which, if we succeed in automatizing SNDICE operations, would monitor with an equivalent precision the optical transmission and the electronic gain of Megacam. On our calibration bench, we are able to explore whether the intrinsic qualities of a multiple LED source can make a calibrated light source more accurate by an order of magnitude than common calibrated photodiodes,
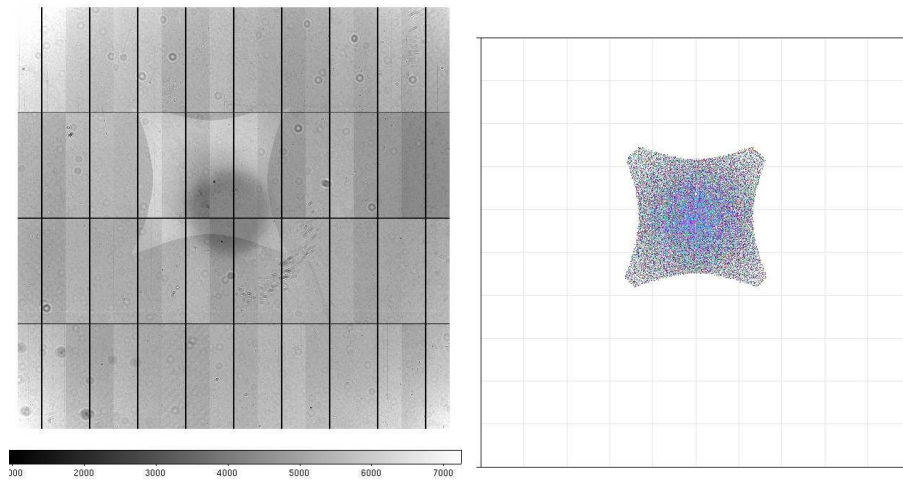
Figure 14. Internal reflexions between the g' filter and the surface of one lens of the Wide Field Corrector: Megacam image (left) and ray tracing simulation (right), reproducing the same 'pincushion' pattern. The ratio of surfaces explains why small reflexion coefficients yield a large effect.

reversing an established hierarchy. We have also problems to solve. For instance, how to deal best with coherent illumination effects.

The second part of our SNDICE achievement is the Cooled Large Area Photodiode and its integrated ultra low current measuring chain, which is able to measure a light flux with a resolution of a few hundredth of electron per second per pixel area. Although this CLAP is operational on our calibration bench, where it is beeing compared to a NIST calibrated photodiode, it has still to be used in situ in the CFHT environment, as planned for the next months.

ACKNOWLEDGMENTS

REFERENCES

[1] Regnault, N., "Photometric Calibration of the Supernova Legacy Survey Fields", ASP Conf. Ser. 364, 587-+ (2007)

[2] Barrelet, E., Juramy, C., "Direct Illumination LED Calibration for Telescope Photometry", Nuclear Inst. and Methods in Physics Research A 585, 93-101 (2008)

[3] Barrelet, E., Lebbolo, H., Sefri, R., "Test of a Low Current Amplifier for a Cooled Large Area Photodiode", LPNHE 2007-04 (2007)

[4] Barrelet, E., Schahmaneche, K., Juramy, C. "Angular Alignment and Control of SNDICE with the Canada-France-Hawaii Telescope", LPNHE 2008-01 (2008)